



Classification of Apnea-Hypopnea Events and Sleep-Wake in Subjects with Obstructive Sleep Apnea

Bijoylaxmi Koley

Assistant professor

Electrical Engineering Department,

B C Roy Engineering College, Durgapur, India

Abstract: This paper presents an automatic method for obstructive sleep apnea screening and sleep (SL) - wake (WA) stages classification based on the whole night PSG (polysomnography) recording of subjects with sleep-disordered breathing during sleep. The proposed algorithm can identify apnea (AP), hypopnea (HY), and Onset of apnea (OA) events within a period of a respiration cycle. In this work, underlying dynamics embedded in each physiological state (i.e., SL, WA) and different pathological events (AP, HY, and OA) are identified with the help of trajectory formed by assigning three signals, i.e., respiration, EEG, and ECG into three orthogonal axes. The spatial distribution of the trajectory is found to be varied with the different stages and different events of OSA subjects. The discriminating information regarding different stages and events is extracted from the spatial distributions by dividing the whole hyperspace into equal-sized subspaces. The persistence of the trajectory in a particular subspace found to be sensitive to the physiological state and different pathological events. Application of standard Bayesian classifier revealed its ability to discriminate different stages. An encouraging detection accuracy of 95.28% is observed across all the subjects.

Index Terms - Apnea-Hypopnea Events, Bayesian classifier, sleep-wake, trajectory.

I. INTRODUCTION

Obstructive Sleep Apnea (OSA) is a sleep disorder characterized by repetitive periods of reduced (hypopnea) or total cessation (apnea) of respiration caused by the partial or complete collapse of the upper airway, respectively [1]. The prevalence of OSA is approximately 4% in adult men and 2% in adult women [2]. The most common sleep apnea symptoms are daytime sleepiness, irritability, tiredness, low concentration, and impaired learning [3].

The undiagnosed OSA is regarded as an essential risk factor for developing severe cardiovascular diseases (e.g., stroke, congestive heart failure, left ventricular hypertrophy, atrial fibrillation, myocardial infarction, and sudden cardiac death) [4]. OSA is commonly treated with continuous positive airway pressure (CPAP), which prevents the upper airway from collapsing. If patients are identified and treated at an early stage of OSA, the adverse health consequences can be reduced [5]. Therefore, early diagnosis of OSA is essential.

The gold-standard method for diagnosing OSA is overnight polysomnography (PSG) (sleep study). This study is carried out in a specialized hospital-based sleep laboratory. In the laboratory, multiple biomedical signals are monitored and recorded during sleep. These signals are; EEG, electrooculography, electromyography, ECG, oronasal airflow, respiratory effort, and oxygen saturation [6]. PSG needs an overnight medical attendant to set up sensors, monitoring, and analysis. According to Rechtschaffen and Kales [7] standard, sleep is broken into two different classes: rapid eye movement (REM) and non-REM sleep. Non-REM is subdivided into four stages: sleep stage 1-4. In PSG, 30s epochs of the signals are used for decision making means sleep staging and events (apnea, hypopnea, leg movement etc.) marking. Using this method of sleep stage scoring and event detection throughout the recording is very tedious, time-consuming work for the physician and depends on the scorer's expertise. The authors [8] reported that manual scoring of each 30s epoch has some degree of variability among highly experienced scorers. Therefore, research on developing reliable, more accurate computerized automatic sleep staging and apnea event detection for subjects with sleep apnea is encouraged. The apnea-hypopnea index (AHI) (e.g., number of apnea and hypopnea events that occur per hour of sleep) from PSG is used to characterize apnea severity. An AHI up to 5 is considered normal, an AHI of 5-15 events/h is mild, an AHI of 15-30 events/h is moderate, and AHI above 30 events/h is severe sleep apnea-hypopnea syndrome [8]. Previous research indicates that apnea events are accompanied by cyclical variations in heart rate: bradycardia/tachycardia [6]. The analysis of Heart Rate Variability (HRV) [9]- and, in addition to HRV, the effect of changes of different ECG-derived parameters, i.e., R-wave duration, ECG pulse energy, the amplitude of S component of each QRS complex, ECG-derived respiration (EDR) [10] during OSA events were studied by the researchers from the past few years. Different researchers in the past implemented several techniques like Hilbert transform, wavelet decomposition, sample entropy method to extract information related to cardiac dynamics from HRV. Features based on RR interval and ECG-derived respiration (EDR) showed 90% correct apnea classification on a minute-by-minute basis [11].

Different computational systems, including the Bayesian hierarchical model, classification and regression method, linear and quadratic classifiers method, neural networks, Support Vector Machine, Deep Neural Network etc. [12-13], were implemented for the automatic detection of OSA events using HRV, EDR and/or ECG signal. The K-nearest neighbor (KNN) classifier [12-14] was employed to distinguish apnea and non-apnea events based on spectral parameters of RR intervals and QRS complex areas. The authors evaluated the KNN-based method through a bivariate autoregressive model [13]. Several researchers directly used the respiration signal to identify apnea events [12], [14].

As OSA causes frequent interruptions in the sleep period during the night, patients cannot achieve good sleep [12]. Such interruptions can be seen as awakening responses in EEG records, and these responses are known as arousals [3]. As this is an area of interest, several studies have been published for automatic detection of arousal using EEG signal. Many researchers have classified OSA events from non-OSA based on the patterns of theta energy ratio in EEG. The study in [15-16] showed that Inter-Hemispheric Synchrony Index (IHSI) computed from EEG could classify apnea with an accuracy of 91%. In recent works, Hilbert-Huang transformation [17] and bi-spectral analysis [18] of EEG are found to be useful for OSA estimation.

Given this background, this current study aims to propose a novel approach for automated recognition of apnea (AP), hypopnea (HY), and onset of apnea (OA) events from regular breathing events and classification of sleep (SL), wake (WA) stages in OSA subjects based on ECG, EEG and respiration signals. A trajectory of multivariate dynamics is estimated in terms of persistence, which correlates with the hidden nonlinear dynamical properties of EEG and the cardio-respiratory system. In past although Bayesian classifier has been applied for detection of sleep apnea [19], however the authors have not detected the above mentioned stages of sleep apnea.

In this work, a trajectory of multivariate dynamics is estimated, which coincides with the underlying nonlinear dynamical features of EEG and the cardio-respiratory system. The persistence of the trajectory in eight areas for all stages/events is thoroughly investigated by getting various statistical metrics. Bayesian classifier has been applied for classification of the multiple statistical metrics and thereafter for automatic identification.

The organization of the paper is as follows. Section II describes the details of the data that has been used in work. The pre-processing of the ECG, EEG, and respiration signals is presented in Section III. Section IV presents the proposed method for trajectory formation and persistence estimation. The Bayesian classifier is presented in Section V. The obtained results are shown in Section VI, followed by a discussion and conclusions in Section VI.

II MATERIALS

In the present study, the signal records of the MIT-BIH PSG database for OSA positive subjects [20] are used, which consist of 18 PSG records from 16 different subjects, with a duration from 1 hour up to 7 hr (4 hr on average), sampled at 250 Hz with 12-bit ADC resolution. All the subjects are male, aged 32 to 56 (average 43), with weights ranging from 89 to 152 kg (mean weight 119 kg). Records include:

- ECG and EEG signals.
- Respiration signals from the nasal thermistor.
- Respiratory effort signals derived by inductance plethysmography
- Blood pressure signals.

The raw data used in this study consist of ECG, EEG, and respiration signals from 14 records of 13 different subjects. The discarded records do not contain respiration signals from nasal thermistor. The website provided the annotation for each recording with an interval of 30s. Onset-of-Apnea (OA) is not marked; hence an epoch (each of the 30s) is considered as an OA epoch that precedes an AP epoch. Total 3771 epochs from non-apneic episodes were collected. Among these epochs, 1792 epochs are from sleep states, including REM and non-REM sleep, and 1979 are from wake states that occur after apnea/hypopnea events. One thousand seven hundred forty-five (1745) epochs from apneic (AP) events, 770 epochs from HY events, and 535 epochs from OA events that are collected from 13 subjects, details of the subjects and stage-wise collected epochs along with subject Identification number (ID) is summarized in Table I.

TABLE I
SUBJECT RECORDS AND DETAILS OF COLLECTED EPOCHS

Records	Subject	SL	WA	AP	HY	OA	Total
slp02a	P1	110	29	81	10	20	250
slp02b	P1	95	90	40	2	23	250
slp03	P2	306	129	34	192	15	676
slp04	P3	162	117	280	1	59	619
slp16	P4	110	278	118	58	33	597
slp32	P5	85	310	73	1	46	515
slp37	P6	34	54	497	0	54	639
slp45	P7	380	5	123	8	82	598
slp48	P8	119	178	128	143	56	624
slp59	P9	110	120	81	70	15	396
slp60	P10	18	191	171	45	80	505
slp66	P11	55	148	12	191	1	407
slp67X	P12	28	50	15	7	9	109
Total		1612	1699	1653	728	493	6185
slp14	P13	180	280	92	42	42	636

III PREPROCESSING OF SIGNALS

The raw signals collected from the database were found to be contaminated with noises from various sources. In the present work, all the three signals ECG, EEG and Respiration were preprocessed separately in different ways to extract the required information and removal of noise.

3.1 ECG Signal Processing

First, the different filters are applied to the ECG signal to remove the noise and artifacts, and then the most represented beat is extracted from each epoch.

Detail frequency-domain study of the ECG signals showed that most of the recordings are contaminated with power line interference of narrowband 60 Hz noise, which is removed with a 6th order IIR notch filter, having a rejection bandwidth of 0.8 Hz. The study also revealed that baseline drift due to respiration is significant and has an average frequency band of 0.18 Hz to 3.74 Hz. To remove the baseline drift and high-frequency noises, the signal is filtered with a bandpass filter of passband 8 to 25Hz. The electrode contact noise and motion artifacts are of high amplitude and duration of 0.1-1s. The recordings are identified by comparing the sampled value with the 200-point moving average value of the signal. The signals of the affected portions are removed and not considered for further processing. Noise due to muscle contraction is of zero mean band-limited, Gaussian type and having very low amplitude concerning ECG signal, hence neglected.

QRS-complex is determined for beat detection from the artifact removed ECG signal using a well-known Hamilton-Tompkins algorithm [21]. After the QRS detection, each beat is extracted by the following technique.

Let $X(n)$ is any epoch of 30s, which was obtained from the artifact removed ECG signal, where $n = 1, 2, 3, \dots, M$ is the sample number, $M = 7500$ for 30s epoch. Now, if $n_{q1}, n_{q2}, n_{q3}, \dots, n_{qm}$ are the sample points on the R peaks, then each beat can be represented as $x_{bi}[s]$, where,

$$s = n_{qi} - (n_{qi} - n_{q(i-1)}) \times 0.6, n_{qi} - (n_{q(i-1)} - n_{q(i-2)}) \times 0.6 + 1, n_{qi} - (n_{q(i-1)} - n_{q(i-2)}) \times 0.6 + 2, \dots, n_{qi} + (n_{q(i+1)} - n_{qi}) \times 0.4$$

If C_{ij} represents correlation between i^{th} beat with j^{th} beat, then

$$C_{ij} = \frac{\sum_{s=1}^N [x_{bi}(s) - \bar{x}_{bi}] [x_{bj}(s) - \bar{x}_{bj}]}{\sum_{s=1}^N [x_{bi}(s) - \bar{x}_{bi}]^{1/2} \sum_{s=1}^N [x_{bj}(s) - \bar{x}_{bj}]^{1/2}}$$

where $\bar{x}_{bi} = \frac{1}{N} \sum_{s=1}^N x_{bi}(s)$, $\bar{x}_{bj} = \frac{1}{N} \sum_{s=1}^N x_{bj}(s)$ and N denotes the average beat length. The most representative beat X_{Bm} for each epoch was obtained by calculating $X_{Bm} = \max[X_B(i)]$. Here, $X_B(i) = \sum_{j=1}^p C_{ij}$, where p is the total number of beat in a particular epoch of 30s. After extracting the most correlated beat it was normalized and up sampled to fit with respiration cycle.

3.2 EEG Signal Processing

The most common physiological artifacts present in the EEG are muscular activity, eye blink, eye movements and ECG. Generally EEG signals are contaminated by ECG signal especially in the time interval of QRS complex. The removal of this noise was done by scaling the ECG channel of polysomnography data to the EEG and subtracted it from the EEG. The ocular artifact zones were removed by visual inspection of the components.

High frequency components can clearly be observed during the waking state. The high-frequency microarousal can be observed after Apnea and Hyponea, whereas, during sleep, the low-frequency signals can be observed. As the apnea and hyponea events occur during sleep therefore extracting the high frequency part and carefully eliminating the low frequency part helped to get a derived EEG signal which vary significantly due to the above mention stages/events. In the present work, the information related to changes in high frequency components of EEG is extracted by the number of times EEG signal crossed the 200 points moving average values taken over a moving window of 200 points. The window is shifted by 1 sample each time. The derived EEG signal hence forth will be termed as *moving-average-EEG* (MAEEG). Fig. 1 shows the wake stage of EEG signal and the 200 points moving average signal for subject P1.

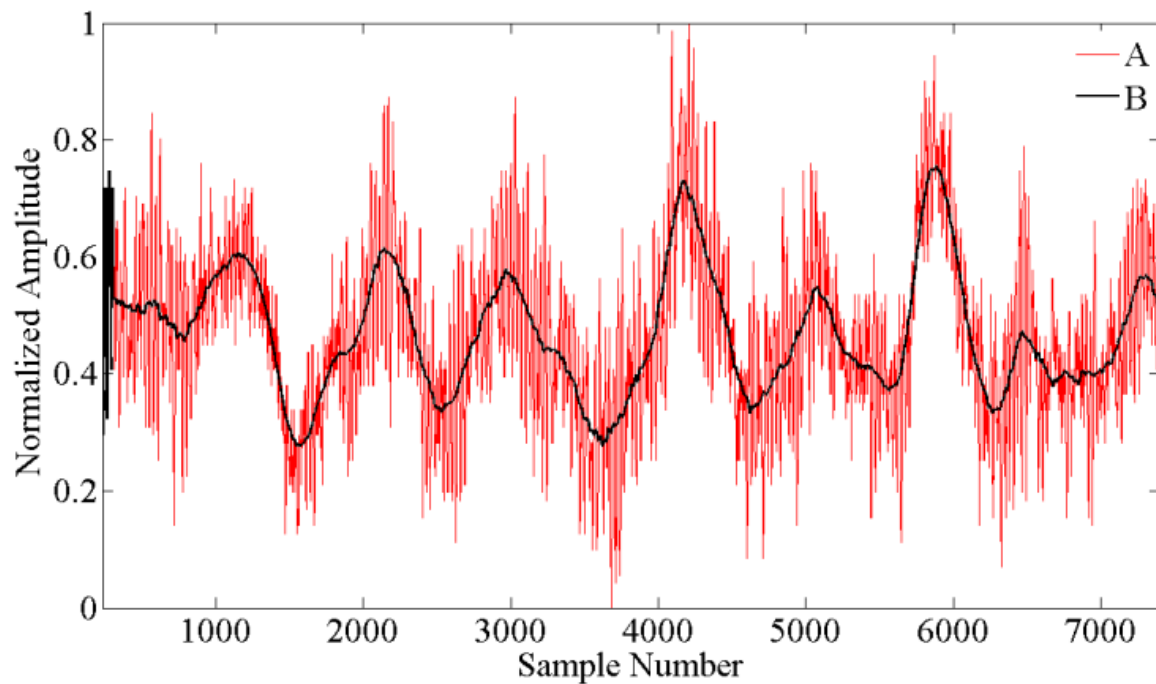


Fig. 1. Time domain plot of A) EEG signal B) 200 point moving average signal.

3.3 Respiration Signal Processing

Respiration signal is of very low frequency compared with ECG and EEG signal and generally having frequency range from 0.18 Hz to 0.42 Hz. In the present work, respiration signal was filtered with 8th order Butterworth filter having cutoff frequency of 3.5 Hz to remove the noise caused by patient or sensor movements.

For extracting a respiration cycle (consists of inspiration and expiration), a zero crossing detection principle with phase transition information was implemented. After separating each cycle the most representative cycle of a particular epoch was obtained as discussed for ECG beats.

IV TRAJECTORY FORMATION WITH ECG, EEG AND RESPIRATION SIGNALS

In order to realize the changes in underlying dynamics of the physiological process, a complete respiration cycle with the corresponding MAEEG signal and the most correlated up sampled ECG beat as shown in Fig. 2 are assigned to three orthogonal axes which results a trajectory in a three-dimensional space.

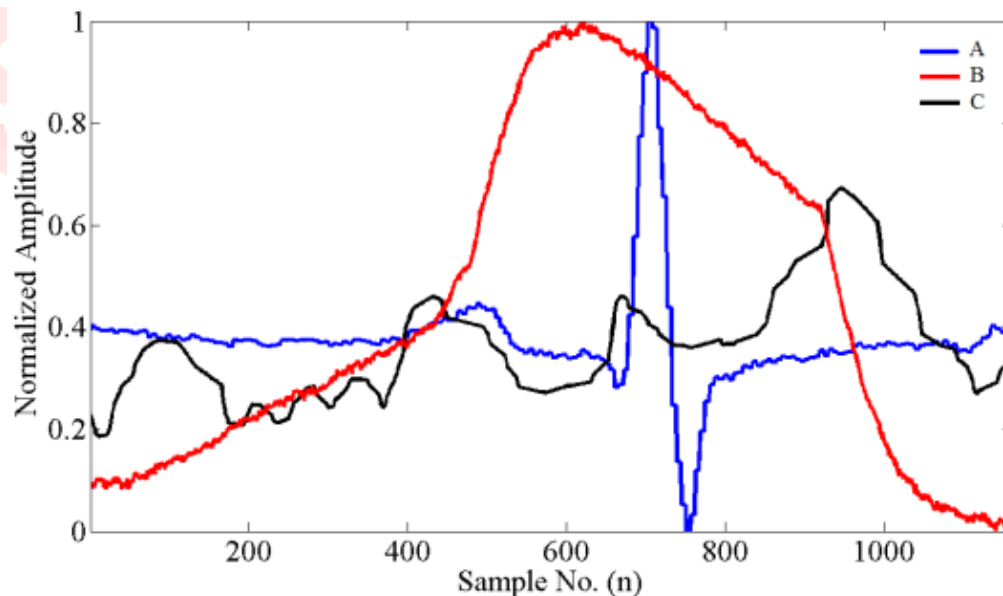


Fig. 2. Time-domain plot of (A) up-sampled ECG signal, (B) Respiration cycle and (C) MACEEG [scaled to fit].

As obstructive apneas and hypopneas alter the linear relationship between autonomic cardiac activity and sleep EEG, From As extensive cross coupling and interaction exists between the cardiovascular and respiratory control system, the traces of the trajectories were found to differ in each physiological state (SL, WA) from normal breathing apnea-hypopnea events vary with the different stages of a subject and also found to vary with subjects. Since the brain activity is very complex in wake stage, EEG signal in this stage shows a complicated random behavior. Since trajectories are found to provide a new way to characterize, describe and quantify the underlying dynamics, therefore, a possible usefulness of it in clinical diagnosis of apnea events and sleep, wake stage classification have been evaluated. Therefore to extract the discriminating information of different stages from these trajectories, the whole space was divided into eight equal-sized subspaces (S1, S2, S3,....., S8) where the persistence (inverse of the total number of point into the particular subspace) of the trajectory in a particular subspace was calculated and a $N \times C$ column matrix was formed where C represents the no of subspaces, whose optimum number found to be 8 and N represents total number

of measurements where each measurement corresponds to each respiration cycle. Fig. 3 describes trace of the trajectory in a three-dimensional space during AP, SL and WA stages of P1 and P2 subjects. The horizontal and vertical slices of Fig. 3 (a) divides the whole space in 8 subspaces. The persistence (total time elapsed) of the trajectory in eight regions for all the different stages/events were studied in details by obtaining various statistical parameters like mean, standard deviation, variance, skewness and kurtosis etc. It was observed that the persistence values in the eight regions for the above mentioned different stages/events are statistically different, but the variations in the statistical properties from subject to subject so dominant that it rejects any straight forward hypothetical rule constructed from the above mentioned statistical properties. In order to provide an overall idea about the variation of statistical properties of the persistence to the readers, a box-whiskers plots for the different stages/events for the eight subspaces is shown in Fig. 4. The box corresponds to the interquartile range, the bar represents the median, and the whiskers extend to the minimum and maximum values the theoretical details about the box-whiskers plots can be found in [22]. Therefore the persistent values in subspaces S1,S2.....S8 were considered as features.

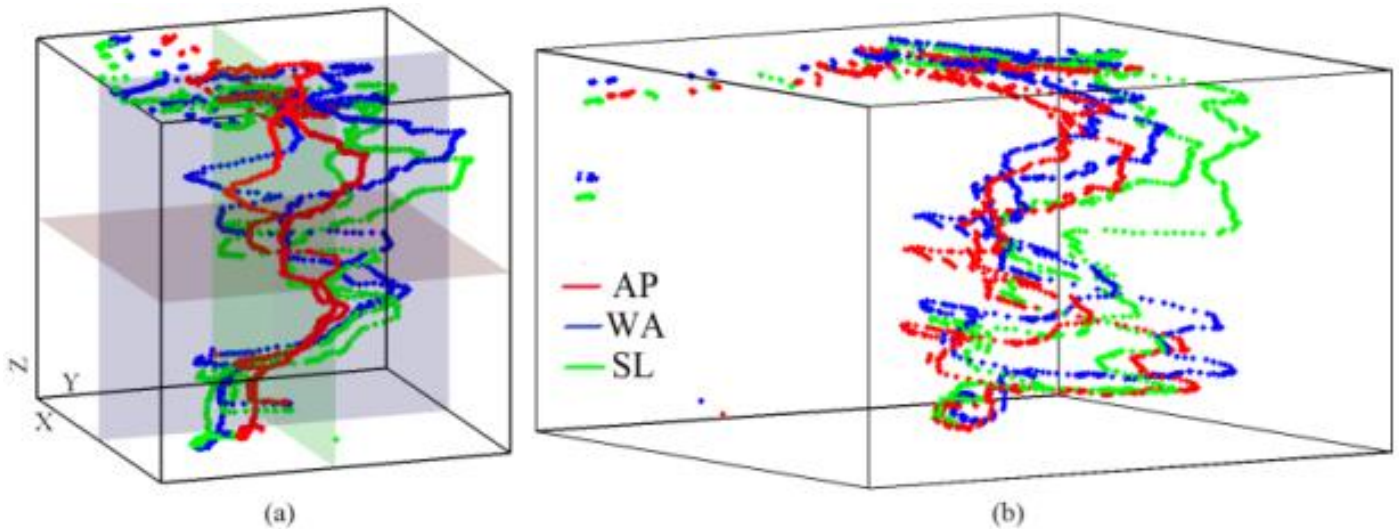


Fig. 3. 3D plot of the trajectory of the ECG, MACEEG and Respiration cycle for AP event and SL, WA stages for subjects: (a) P1 and (b) P2.

V CLASSIFICATION BASED ON BAYES' RULE

The objective of the Bayesian classifier [22] is to find the class which has the maximum posterior probability for a given observation. Mathematically for a particular class c where, $c = \{1, 2, \dots, C\}$ using Bayesian classification one finds:

$$\hat{C} = \arg \max_{1 \leq c \leq C} P(\theta_c | X) = \arg \max_{1 \leq c \leq C} \frac{p(X | \theta_c) P(\theta_c)}{p(X)},$$

where $p(X | \theta_c)$ represents class conditional probability, $P(\theta_c)$ prior probability and $p(X)$ unconditional density, which is independent of class. Using logarithms and considering the independence between observations, the classification system becomes,

$$\hat{C} = \arg \max_{1 \leq c \leq C} \sum_{n=1}^N \ln \{p(\vec{x}_n | \theta_c) P(\theta_c)\}$$

where $p(\vec{x}_n | \theta_c)$ is given in equation (8).

VI RESULTS AND DISCUSSION

A complete experimental evaluation is performed on 12-subject to develop a Bayesian multiclass classifier. Initially, evaluation was done on the subject-wise dataset by training and testing the Bayesian classifier with the feature vectors of the same subject. In this case, the features are drawn randomly from the respective subject-wise dataset of a particular subject, and the rest of the features of that patient are used for testing. The performance of the classifier is studied by varying the training data size. Table VI summarizes the classifier performance. It showed that in most cases, 100% successful classification is obtained with the training data size of 80%. This outstanding performance is because subject-wise feature space is often not overlapped, and a clear decision boundary can be formed.

TABLE II
SUCCESSFUL CLASSIFICATION IN (%) FOR INDIVIDUAL SUBJECT-WISE TRAINING AND TESTING

Patient ID	Training Data Size (%)		
	80	70	60
P1	100	99.6	98.8
P2	100	100	99.4
P3	98.9	98.7	98.6
P4	100	100	99.3
P5	100	99.4	98.6
P6	100	99.8	99.3
P7	98.6	97.8	97.1
P8	99.4	99.1	98.7
P9	100	100	98.7
P10	100	99.9	99.5
P11	99.5	98.9	98.2
P12	100	100	99.7
Average	99.7	99.4	98.8

In the next stage of the evaluation process, the Bayesian classifier is trained with a dataset of all the subjects (P1 to P12) by randomly drawing the training features from all the subjects while remaining used for testing. Varying training data sizes perform the detailed study. The evaluation results presented in Table III are the classification performance with 70% training data size. In this case, among the total 6185 (as listed in Table I) no feature vectors, 4328 (~70%) feature vectors are randomly selected for training, and the remaining 1857 feature vectors are kept for testing. The actual number of feature vectors in each AP, SL, WA, HY, and OA stage are 484, 510, 496, 218, and 149, respectively. After training of Bayesian classifier, a cross-validation scheme is adopted for multiple runs to evaluate the generalization ability of the classifier. The procedure is summarized in Table III in a well-known confusion matrix. From this confusion matrix, it can be observed that the mean value of correct classification for AP, SL, WA, HY, and OA stages are 459, 498, 492, 210, and 134, respectively, where ± 11 , ± 4 , ± 2 , ± 7 and ± 6 indicate the maximum deviation over all the run. The average successful classification by the Bayesian classifier, with 70%, 80%, and 90% training data sizes, are $96.06 \pm 1.6\%$, $96.88 \pm 0.9\%$, and $97.72 \pm 0.5\%$, respectively. The dropped in the classifier performance is found when compared to subject-wise classification because the subject-wise features are often separable by linear or nonlinear decision boundaries. Still, as individual subjects have unique patterns of ECG, EEG, and respiration signals, their feature vectors vary in feature space. By considering the features of all the subjects, it was observed that the features of different classes (i.e., SL, AP, HY, OA) overlapped with each other.

The performance of the classifier is analyzed by calculating False Negative (FN), False Positive (FP), True Positive (TP), and True Negative (TN) with the help of the confusion matrix shown in Table IV. From that, Sensitivity (SE), Specificity (SP), Predictivity (PR), and Accuracy (AC) were calculated according to [22], which is shown in Table IV. It can be observed that the Sensitivity of the OA class is the lowest among all the classes, which is because OA class features are overlapped with SL and AP classes. In contrast, the AP has the most insufficient accuracy.

TABLE III
CONFUSION MATRIX FOR SUBJECT INDEPENDENT CLASSIFICATION WITH 70% TRAINING DATA SIZE

		Predicted Class				
		AP	SL	WA	HY	OA
True Class	AP	459 \pm 11	0	0	15 \pm 7	10 \pm 4
	SL	0	498 \pm 4	0	0	12 \pm 4
	WA	0	4 \pm 2	492 \pm 2	0	0
	HY	15 \pm 5	0	0	201 \pm 7	2 \pm 2
	OA	7 \pm 3	7 \pm 2	0	1 \pm 1	134 \pm 6

TABLE IV
VARIOUS PARAMETERS FOR CLASSIFIER PERFORMANCE EVALUATION

FN	FP	TP	TN	SE	SP	PR	AC
25	22	459	1351	0.948	0.984	0.955	0.975
12	11	498	1336	0.976	0.992	0.979	0.988
4	0	492	1361	0.992	1.000	1.000	0.998
17	17	201	1622	0.923	0.990	0.924	0.982
15	24	134	1683	0.900	0.986	0.849	0.979

In a practical situation, the classifier has to face new features of the new subjects whose characteristics are not included in the construction of the model. Leave-one-out cross-validation technique may not reflect the classification accuracy in that case because the features from all these 12 subjects are taken to develop the model. For that, the record of P13, which is kept separately and not used for the model's design, is used only for testing the performance. In this case, the model is trained with all the data sets from 12 patients. The confusion matrix shown in Table V summarizes the obtained results with the Bayesian classifier. The successful classification that is achieved with the achieved with Bayesian classifier is 95.28 %.

TABLE V
CONFUSION MATRIX FOR CLASSIFICATION OF UNKNOWN SUBJECT (P13)

		Predicted Class				
		AP	SL	WA	HY	OA
True Class	AP	168	0	0	7	5
	SL	0	271	0	2	7
	WA	0	0	92	0	0
	HY	3	0	0	39	0
	OA	3	3	0	0	36

Another analysis is performed to find the optimum number of subspaces. That is obtained experimentally by varying the number of subspaces from 4 to 32. Finally, the optimum number is decided as eight, with a tradeoff between classifier performance and computational requirements.

VI CONCLUSION

The new technique for extraction features from ECG, Respiration, and EEG signals is reasonable for classifying different stages in OSA subjects. The method is reasonably fast as it samples the signal only for 30 seconds and analyzes the signal only for one respiration cycle compared to the algorithm based on HRV. The highest sensitivity achieved by the model is 99% in the subject-wise dataset and 97% in the case of the dataset formed with all the subjects. Leave-one-out cross-validation scheme was found to be better when compared to other algorithms. Most of the errors are due to misclassification in HY and OA classes, in a practical situation that is also difficult to separate. When a completely unknown subject was presented to the model, 95.28% successful classification was obtained. It proves the acceptance of the proposed model for classification.

REFERENCES

- [1] American Academy of Sleep Medicine (AASM) Task Force, "Sleep-related breathing disorders in adults: Recommendations for syndrome definition and measurement techniques in clinical research," *Sleep*, vol. 22, pp. 667–689, Aug. 1999.
- [2] M. E. Tagluk, M. Akin, and N. Sezgin, "Classification of sleep apnea by using wavelet transform and artificial neural networks," *Expert Systems with Applications*, vol. 37, pp. 1600-1607, 2010.
- [3] D. P. White, "Sleep Apnea," *Proc. Amer. Thorac. Soc.*, vol. 3, pp. 124-128, 2006.
- [4] J. Coleman, "Complications of snoring, upper airway resistance syndrome, and obstructive sleep apnea syndrome in adults," *Otolaryngol. Clin. North Amer.*, vol. 32, pp. 223-234, 1999.
- [5] T. Young, P. Peprad, M. Palta, K. M. Hla, L. Finn, B. Morgan, and J. Skatrud, "Population-based study of sleep-disordered breathing as a risk factor for hypertension," *Arch. Intern. Med.*, vol. 157, pp. 1746-1752, 1997.
- [6] T. Young, M. Palta, J. Dempsey, J. Skatrud, S. Weber, and S. Badr, "The occurrence of sleep-disordered breathing among middle-aged adults," *N. Engl. J. Med.*, vol. 328, pp. 1230–1235, 1993.
- [7] Rechtschaffen & Kales, "A manual of standardized terminology, techniques and scoring system for sleep stages of human subjects", standard. Psychiatry and clinical neurosciences, 55(3), pp.305-310, 1968.
- [8] Alvarez-Estevez D, Rijsman RM., "Computer-assisted analysis of polysomnographic recordings improves inter-scorer associated agreement and scoring times", medRxiv. 2022.
- [9] Li, Yifan, Weifeng Pan, Kunyang Li, Qing Jiang, and Guanzheng Liu. "Sliding trend fuzzy approximate entropy as a novel descriptor of heart rate variability in obstructive sleep apnea." *IEEE journal of biomedical and health informatics* 23, no. 1 (2018): 175-183.
- [10] Ali, Syeda Quratulain, Sohail Khalid, and Samir Brahim Belhaouari. "A Novel Technique to Diagnose Sleep Apnea in Suspected Patients Using Their ECG Data." *IEEE Access*, No. 7 (2019): 35184-35194.
- [11] F. Mendonça, S. S. Mostafa, A. G. Ravelo-García, F. Morgado-Dias and T. Penzel, "A Review of Obstructive Sleep Apnea Detection Approaches," in *IEEE Journal of Biomedical and Health Informatics*, vol. 23, no. 2, pp. 825-837, March 2019, doi: 10.1109/JBHI.2018.2823265.
- [12] S. Ahmadzadeh, J. Luo and R. Wiffen, "Review on Biomedical Sensors, Technologies and Algorithms for Diagnosis of Sleep Disordered Breathing: Comprehensive Survey," in *IEEE Reviews in Biomedical Engineering*, vol. 15, pp. 4-22, 2022, doi: 10.1109/RBME.2020.3033930.
- [13] Ramachandran A, Karupiah A. "A Survey on Recent Advances in Machine Learning Based Sleep Apnea Detection Systems", *Healthcare (Basel)*. 2021 Jul 20;9(7):914. doi: 10.3390/healthcare9070914. PMID: 34356293; PMCID: PMC8306425.
- [14] Mostafa, Sheikh Shanawaz, Fábio Mendonça, Antonio G Ravelo-García, and Fernando Morgado-Dias. "A systematic review of detecting sleep apnea using deep learning." *Sensors* 19, no. 22 (2019): 4934.
- [15] N. Parekh, B. Dave, R. Shah and K. Srivastava, "Automatic Sleep Stage Scoring on Raw Single-Channel EEG : A comparative analysis of CNN Architectures," 2021 Fourth International Conference on Electrical, Computer and Communication Technologies (ICECCT), 2021, pp. 1-8, doi: 10.1109/ICECCT52121.2021.9616895.
- [16] Wang, Yao, Zhuangwen Xiao, Shuaiwen Fang, Weiming Li, Jinhai Wang, and Xiaoyun Zhao. "BI-Directional long short-term memory for automatic detection of sleep apnea events based on single channel EEG signal." *Computers in biology and medicine* (2022): 105211.
- [17] Zhang, Junming, Ruxian Yao, Wengeng Ge, and Jinfeng Gao. "Orthogonal convolutional neural networks for automatic sleep stage classification based on single-channel EEG." *Computer methods and programs in biomedicine* 183 (2020): 105089.
- [18] Rakhonde, Mayuri A., Kishor P. Wagh, and Ravi V. Mante. "Survey on Sleep Stage Scoring Techniques using Feature Discovery." In 2020 4th International Conference on Computer, Communication and Signal Processing (ICCCSP), pp. 1-3. IEEE, 2020.
- [19] D. Ferreira-Santos and P. P. Rodrigues, "Improving Diagnosis in Obstructive Sleep Apnea with Clinical Data: A Bayesian Network Approach," 2017 IEEE 30th International Symposium on Computer-Based Medical Systems (CBMS), 2017, pp. 612-617, doi: 10.1109/CBMS.2017.19.
- [20] G. Goldberger et al., "Physiobank, physiobank, and physionet: Components of a new research resource for complex physiologic signals," *Circulation*, vol. 101, no. 23, pp. 215-220, 2000.
- [21] P. S. Hamilton and W. J. Tompkins, "Quantitative investigation of QRS detection rules using the MIT/BIH Arrhythmia database," *IEEE Trans. Biomed. Eng.*, vol. BME-33, no. 12, pp. 1157-1165, Dec. 1986.
- [22] J. P. Marques de Sa, *Applied Statistics using Spss, Statistica, Matlab and R*. 2nd ed. Springer, Berlin Heidelberg New York, 2007.
- [23] N. F. Garcia, P. Gomis, A. La Cruz, G. Passeriello, and F. Mora, "Bayesian hierarchical model with wavelet transform coefficients of the ECG in obstructive